Mecánica Computacional Vol. XXI, pp. 1998–2008
S. R. Idelsohn, V. E. Sonzogni and A. Cardona (Eds.)
Santa Fe–Paraná, Argentina, October 2002

NUMERICAL ANALYSIS OF THE EUROCODE ASSUMPTIONS FOR TEMPERATURE DISTRIBUTION IN COMPOSITE STEEL AND CONCRETE BEAMS

Ricardo H. Fakury*, Estevam B. Las Casas*, Fernando P. F. Júnior*, and Laura M. P. Abreu†

* Department of Structural Engineering
Federal University of Minas Gerais
Belo Horizonte, Minas Gerais, Brazil
e-mail: posees@dees.ufmg.br, web page: http://www.dees.ufmg.br

† Codeme Engenharia
Betim, Minas Gerais, Brazil
e-mail: codeme@codeme.com.br, web page: http://www.codeme.com.br

Key words: Composite beams, Fire design, Eurocode, Finite Element Method.

Abstract. *The design of composite steel and concrete beams should normally include the progressive deterioration in strength and stiffness of its components (steel section, concrete slab and shear connectors) with temperature rise under fire. In European Prestandard Eurocode 4, a simple calculation method is described where the assessment of the composite beam strength consists of two different steps: first the calculation of temperature distribution versus time in the cross-section and then the determination of the mechanical behavior to estimate the load-bearing capacity of the member.*

In this work, a study is described to verify if the simplifications allowed by Eurocode 4 to obtain the temperature rise in the components of composite beams comprising steel beams with no encasement may lead to inappropriate design. Two programs were developed for the analysis: the first, a heat transfer code, for the determination of the temperature distribution in each region of the composite beam; the second, a structural analysis program, for designing the composite beam. As an example, a composite beam has its positive bending moment strength determined under the temperature calculated numerically as well as the temperature obtained with the simplifications. The strength results are compared and discussed.

1 INTRODUCTION

The prestandard Eurocode 4 [1] proposes a simplified approach to the design of composite beams comprising steel beams with no encasement under fire, which includes:

- the determination of the temperature distribution at the cross section of the steel beam (in case it is unprotected or insulated by fire protection material using hollow or contour encasement), as well as at the concrete slab and shear connectors;
- the determination of the design bending moment and shear strengths for the composite beam at high temperature, considering the decay of the mechanical properties of the involved materials with the increase in temperature;
- the comparison of the design bending moment and shear strengths with the corresponding design effect of actions, calculated considering the recommendations of Eurocode 1 [2] for the fire design.

Composite beams should include class 1 or class 2 I beam cross-section in Eurocode 3 [3] (for simply supported beams, the compressed steel flange of class 3 may be treated as class 2, provided it is connected to the concrete slab by shear connectors). The concrete slab can be either a flat slab or a composite slab with profiled steel sheets, and the shear connectors should be either stud bolts or laminated U shapes. As for the determination of the temperatures, Eurocode 4 [1] allows the following simplifications:

- For steel beams with contour encasement fire protection or unprotected, the bottom flange temperature can be determined as if it were subjected to fire on all four sides. For the top flange, the temperature can be assumed to be acting on three sides;
- still for steel shapes with contour encasement protection or unprotected, web temperature can be taken as the average between the temperatures for the flanges in case of sections with height equal or lower to 400 mm. For higher height values, web temperature can be taken as equal to the temperature at the bottom flange;
- concrete slab temperature can be taken as 40% of the upper flange in the calculation of the decrease in concrete strength for the design of the shear connectors;
- the temperature of the shear connectors can be taken as 80% of the temperature at the top flange.

In the following items the implications of these simplifying hypotheses are evaluated for the usual case of contour encasement fire protection, using a finite element heat transfer code and subsequently a design code for composite beams under fire, both developed specifically for this type of analysis. A composite simply supported beam with dimensions within usual bounds in buildings, flat concrete slab and stud bolt shear connectors has its bending moment strength determined under simplified and calculated temperature distributions for ISO 834 [4] fire of 30, 60, 90 and 120 minutes duration, and the results are compared and critically discussed.

2 EUROCODE 4 SUGGESTED PROCEDURE

2.1 General Aspects

The composite beam should withstand the loading for a time *t* under fire, without reaching ultimate limit state. During this time, the heating of the cross section will occur having as reference the temperature of the gases at the compartment, described by the standard fire curve, as defined in ISO 834.

2.2 Steel section

The heat distribution in the unprotected and with encasement fire protection steel section can be taken as non-uniform, with the cross section divided in three independent parts - top flange, web and bottom flange. Eurocode 4 Part 1.2 [1] proposes:

- a procedure for the determination of the temperature at upper and lower flange;
- that the temperature of the web be considered as equal to temperature at the top flange for steel sections with height equal or higher than 400 mm, or equal to the temperature at the bottom flange for sections with height of more than 400 mm;
- the use of listed values for factors $k_{y,\theta}$ and $k_{E,\theta}$, as shown in figure 1, to reduce the steel yield strength f_y and Young's modulus E.

2.3 Concrete slab

The variation of the temperature is assumed to occur only through the thickness of the slab, under the assumption of incidence of fire in its lower surface. This variation is defined in Eurocode 4 [1]. For example, in a 100 mm thickness slab, subjected during 30 minutes to standard fire, temperature varies from 535°C at the lower surface to 60°C at the upper surface, while for 120 minutes the temperatures range from 800°C to 210°C.

The increase in temperature leads to a decrease in the concrete compressive strength f_{ck}, and elasticity modulus, E_c, according to the reduction factors $k_{c,\theta}$ and $k_{Ec,\theta}$, given by Eurocode 4 and shown in figure 1.

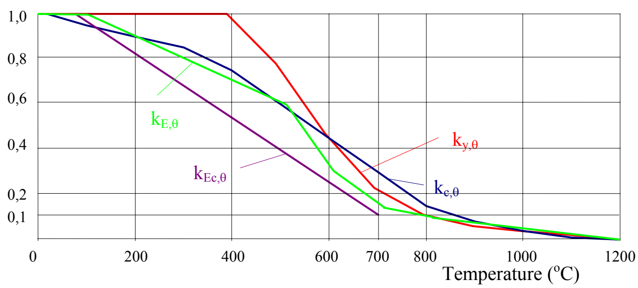

Figure 1- Reduction factors for steel and concrete in strength and elasticity modulus.

2.4 Shear connectors

For the determination of the resistance of shear connectors for collapse of the concrete slab, the compressive characteristic strength of concrete at room temperature f_{ck} is multiplied by $k_{c,\theta}$, while the concrete elasticity modulus at room temperature E_c is multiplied by $k_{Ec,\theta}$ obtained for a temperature of 40% of the temperature at the top flange of the steel section. For the hypothesis of collapse of the shear connector, a reduction factor given by $k_{y,\theta}$ is applied to the steel's limit strength at room temperature f_u reduced by factor $k_{y,\theta}$ as mentioned in item 2.2, for 80% of the temperature at the steel beam top flange. Factors $k_{c,\theta}$ and $k_{Ec,\theta}$ are the same as mentioned in 2.3, and $k_{y,\theta}$ in 2.2.

2.5 Hogging moment resistance

The design value of the hogging moment resistance under fire, $M_{fi,Rd}$, should be calculated by the plastic theory, considering the variation of mechanical properties with temperature.

3 TEMPERATURE DISTRIBUTION BY FEM

3.1 Basic equations

The starting point is Poisson's Equation:

$$\rho c \frac{\partial \theta}{\partial t} = \nabla^2 \boldsymbol{D}\theta + \rho r \quad in\ \Omega \tag{1}$$

where θ is the temperature, t time , ρ material density, c specific heat, ρr tdensity due to an external source and $\boldsymbol{D}$ the constitutive matrix, which includes tthermal conductivities λ for the different dimensions of the domain. Matrix $\boldsymbol{D}$ for a two-dimensional domain is given by (2).

$$\boldsymbol{D} = \begin{bmatrix} \lambda_x & 0 \\ 0 & \lambda_y \end{bmatrix} \tag{2}$$

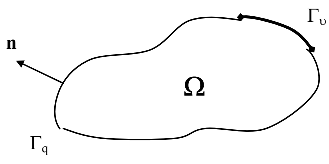

Figure 2 – Boundary conditions on 2D

The boundary conditions for the problem are shown in Figure 2, and can be described as:

- Dirichlet type, with θ given for part of the boundary:

$$\theta - \bar{\theta} = 0 \;\; in \;\; \Gamma_\theta \tag{3}$$

- Neumann condition, for a fixed temperature gradient normal to the surface:

$$\boldsymbol{n}^T \boldsymbol{q} + \alpha(\theta_f - \theta_s) + \bar{\boldsymbol{q}} = 0 \;\; in \;\; \Gamma_q \tag{4}$$

In the previous equations, $\bar{\theta}$ is the fixed value for the temperature in the domain, α stands for the convection-radiation coefficient, $\bar{\boldsymbol{q}}$ is the temperature flux, known at the boundary, θ_f is the temperature for the gas at the boundary, $\boldsymbol{n}$ is the normal vector and $\boldsymbol{q}$ is the temperature gradient vector, given by:

$$\boldsymbol{n} = \begin{bmatrix} n_x & n_y \end{bmatrix}^T \tag{5}$$

$$\boldsymbol{q_n} = \lfloor q_x \quad q_y \rfloor = -\boldsymbol{D}\nabla\theta \tag{6}$$

where the gradient operator is defined by:

$$\nabla = \begin{bmatrix} \frac{\partial}{\partial x} & \frac{\partial}{\partial y} \end{bmatrix}^T \tag{7}$$

Depending on the values for the parameters in equation (4), the following cases are represented:

- isolated boundary: no flux at the boundary, resulting in $\boldsymbol{n}^T = 0$ as $\bar{\boldsymbol{q}} = 0$ and $\alpha = 0$;
- prescribed boundary flux: $\boldsymbol{n}^T\boldsymbol{q} = -\bar{\boldsymbol{q}}$ as $\alpha = 0$;
- boundary with heat transfer by convection or radiation: in this case, $\boldsymbol{n}^T\boldsymbol{q} = -\alpha\,(\theta_f - \theta_s)$, as $\bar{\boldsymbol{q}} = 0$.

Factor α groups the effect of radiation and convection, and is given by:

$$\begin{aligned} \alpha = h + \varepsilon_{res}\sigma\, [81385668 + 447174(\theta_f + \theta_s) + (\theta_f + \theta_s)(\theta_f^{\,2} + \theta_s^{\,2}) + \\ + 1092(\theta_f^{\,2} + \theta_f\,\theta_s + \theta_s^{\,2})] \end{aligned} \tag{8}$$

where:

- α_c is the convection heat trai sfer coefficient, which, according to Eurocode 4 [1], can be taken as 25 W/m^2 ^{o}C ;
- ε_{res} is the emissivity between gases and surface, which can be taken as 0.5, according to [1];
- σ is the Stefan-Boltzmann's constant (equal to 5.669x10^{-8} W/m^{2}K^4);
- θ_f is the temperature of the gases (^{o}C);
- θ_s is the temperature for the surfaces (^{o}C).

3.2 Formulation

The functional representing the problem can be obtained using the weighted residuals method applied to equation (1), using boundary condition (4). The resulting integral equation [6] is given by:

$$\int_{\Omega}\left[\nabla^{T}\boldsymbol{D}\nabla\theta+\rho r\right]\partial\Omega-\int_{\Omega}\rho c\frac{\partial\theta}{\partial t}\partial\Omega+\oint_{\Gamma_q}\left[\boldsymbol{n}^{T}\boldsymbol{D}\nabla\theta+\alpha(\theta_f-\theta_s)+\overline{\boldsymbol{q}}\right]\partial\Gamma_q=0 \tag{9}$$

After integrating the term $\nabla^{T}\boldsymbol{D}\,\nabla\theta$ and rearranging the terms, the result is:

$$\begin{aligned}&\int_{\Omega}\boldsymbol{W}^{T}\rho c\frac{\partial\theta}{\partial t}\partial\Omega+\int_{\Omega}\nabla^{T}\boldsymbol{W}^{T}\boldsymbol{D}\nabla\theta\partial\Omega+\oint_{\Gamma_q}\boldsymbol{W}^{T}\alpha\theta\partial\Gamma_q=\\&\int_{\Omega}\boldsymbol{W}^{T}\rho r\partial\Omega-\oint_{\Gamma_q}\boldsymbol{W}^{T}\overline{\boldsymbol{q}}_{\boldsymbol{n}}\partial\Gamma_q+\oint_{\Gamma_q}\boldsymbol{W}^{T}\alpha\theta_f\partial\Gamma_q-\oint_{\Gamma_\theta}\boldsymbol{W}^{T}\boldsymbol{q}_{\boldsymbol{n}}\partial\Gamma_q\end{aligned} \tag{10}$$

3.3 Discretization

The usual finite element approximation is used, as indicated in (11), where N_i are the shape functions and $\boldsymbol{a}^{(e)}$ the nodal variables (temperatures):

$$\theta=\sum N_i\theta_i=\boldsymbol{Na}^{(e)} \tag{11}$$

As for the gradient vector for each element,

$$\boldsymbol{g}=\nabla\theta=\nabla\boldsymbol{Na}^{(e)}=\boldsymbol{Ba}^{(e)} \tag{12}$$

where $\boldsymbol{B}=\left[\mathrm{B}_1,\ldots,\mathrm{B}_n\right]$, with $B_i=\begin{bmatrix}\dfrac{\partial N_i}{\partial x} & \dfrac{\partial N_i}{\partial y}\end{bmatrix}^{T}$ for 2D problems.

The flux vector can be calculated based on the nodal variables:

$$\boldsymbol{q}=-\boldsymbol{DBa}^{(e)} \tag{13}$$

Using the results given in equations (11) and (12) in (10), and taking the weighting factor $\boldsymbol{W}$ equal to $\boldsymbol{N}$, the resulting system of equations is:

$$\boldsymbol{M}\frac{\partial\boldsymbol{a}}{\partial t}+\boldsymbol{Ka}=\boldsymbol{f} \tag{14}$$

In equation (14) $\boldsymbol{M}$ and $\boldsymbol{K}$ are the mass and stiffness matrixes, $\boldsymbol{a}$ is the vector of unknowns and $\boldsymbol{f}$ is the force vector, as described in equations (15) to (17):

$$\boldsymbol{M}^{(e)}=\int_{\Omega^{(e)}}\rho c\boldsymbol{N}^{T}\boldsymbol{N}\partial\Omega^{(e)} \tag{15}$$

$$\boldsymbol{K}^{(e)}=\int_{\Omega^{(e)}}\boldsymbol{B}^{T}\boldsymbol{DB}\partial\Omega^{(e)}+\alpha\oint_{\Gamma_q^{(e)}}\boldsymbol{N}^{T}\boldsymbol{N}\partial\Gamma_q^{(e)} \tag{16}$$

$$\boldsymbol{f}^{(e)} = \int_{\Omega^{(e)}} \boldsymbol{N}^T \rho r \partial\Omega^{(e)} - \oint_{\Gamma_q^{(e)}} \boldsymbol{N}^T \overline{\boldsymbol{q}} \partial\Gamma_q^{(e)} + \oint_{\Gamma_q^{(e)}} \boldsymbol{N}^T \alpha\theta_f \partial\Gamma_q^{(e)} - \oint_{\Gamma_\theta^{(e)}} \boldsymbol{n}^T \boldsymbol{N}^T \boldsymbol{q}_{\boldsymbol{n}} \partial\Gamma_\theta^{(e)} \tag{17}$$

For the steady state solution, the problem simplifies to:

$$\boldsymbol{Ka} = \boldsymbol{f} \tag{18}$$

From the determination of the nodal temperatures, their gradients and heat flux can be determined by equations (12) and (13). For transient problems, the solution requires the integration of equation (14) in time. The use of a generalized finite difference trapezoidal rule leads to:

$$\left[\frac{\boldsymbol{M}}{\Delta t} + \beta\boldsymbol{K}\right]\boldsymbol{a}_t = \beta\boldsymbol{f}_t + (1-\beta)\boldsymbol{f}_{t-1} + \left[\frac{\boldsymbol{M}}{\Delta t} - (1-\beta)\boldsymbol{K}\right]\boldsymbol{a}_{t-1} \tag{19}$$

where β is given by:

$$\boldsymbol{a}_\beta = \beta\,\boldsymbol{a}_t + (1-\beta)\boldsymbol{a}_{t-1} \tag{20}$$

The integration scheme is conditionally stable, requiring the use of $\beta \geq 0.5$. The value $\beta = 1$ is used in this work.

4 CASE STUDY

The composite beam used in this analysis combines a welded I section 400 x 58 (400 x 200 x 12.5 x 6.3) with no concrete encasement and a 100 mm thickness flat concrete slab with effective width equal to 1800 mm. The steel has yield strength of 250 MPa and the concrete compressive characteristic strength of 18 MPa. The shear connectors are stud bolts with 19 mm diameter, 80 mm height and ultimate strength of 415 MPa.

Temperature distribution in the cross section of the beam was determined with a transient non-linear analysis, using a special purpose program based on the CALTEP platform (Zarate and Oñate [5]), which received a transient non-linear modulus and the inclusion of the possibility to consider radiation boundary conditions and the standard fire curve given in ISO 834 [4].

The standard curves for fire duration of 30, 60, 90 and 120 minutes were considered in the determination of the contour protected steel beam temperatures. The following points (Figure 3) where analyzed: (i) points 1, 2 and 3 in the steel beam, respectively at the centers of gravity of the bottom flange, web and top flange; (ii) point 4, placed at the vertical axis of the shear connector, at a height of 19 mm (equal to its diameter), and (iii) point 5 at the concrete slab, coinciding with the vertical axis of the composite beam, at an elevation from the lower surface of the slab equal to the semi-height of the shear connector (40 mm). Temperature at point 4 was used as reference for the determination of the shear connector ultimate strength, and point 5 at the slab for defining the concrete resistance in the region of the shear connectors. Temperatures at elevations 1 to 4 along the thickness of the slab were also calculated.

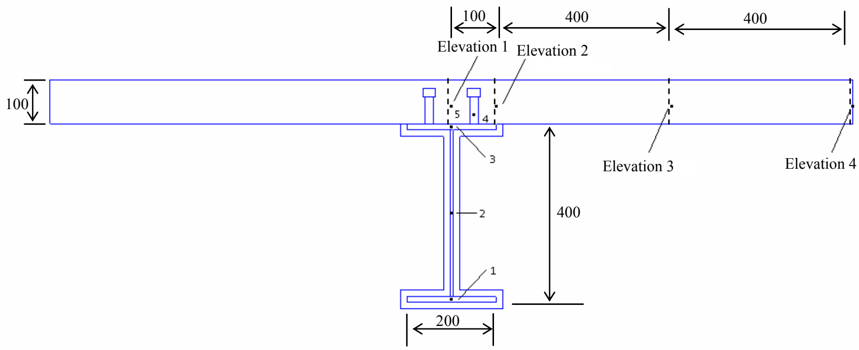

Figure 3 – Points analyzed in composite beams

The fire protection considered in the analysis was a 15 mm thickness sprayed vermiculite gypsum plaster. The thermal properties of the materials are given in Table 1.

Table 1- Thermal properties of the materials

	Thermal conductivity (W/m °C)	Specific heat (J/kg °C)	Density (kg/m^3)
Steel	45.0	600	7850
Concrete	0.90	1000	2400
Protection material	0.15	1100	350

Figure 4 shows a sample result of the program, for fire duration of 30 and 120 minutes.

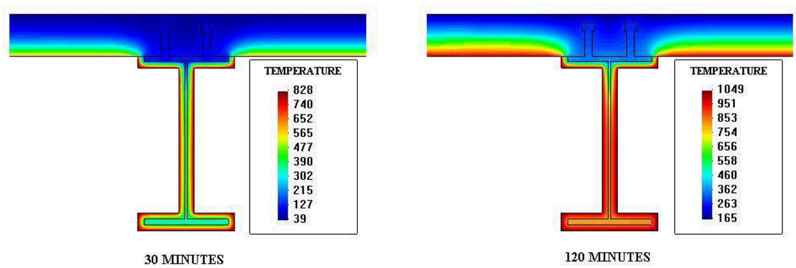

Figure 4 – Temperature distribution on the composite beam

Temperatures at points 1 to 5 are listed in table 2, as well as the ratios between the temperatures at the connector (point 4) and the top steel beam flange (point 3) and between the temperatures at the slab (point 5) and top steel beam flange (point 3).

Table 2 - Temperature at points 1 to 5 (Figure 3)

		Temperature (°C)			
Location	Point	30 min	60 min	90 min	120 min
Steel section	1	347	552	698	815
	2	398	617	749	833
	3	132	225	307	376
Connector	4	101	186	260	325
Slab	5	66	136	208	271
θ_4/θ_3		0.77	0.83	0.85	0.86
θ_5/θ_3		0.50	0.60	0.68	0.72

Table 3 lists the temperatures at different elevations at the flat concrete slab.

Table 3 – Temperature at elevations 1 to 4 (Figure 3) in the concrete slab.

		Temperature (°C)										
Time (min)	Elevation	Elevation referred to lower slab surface (mm)										
		0	10	20	30	40	50	60	70	80	90	100
30	1	130	104	80	74	66	60	55	51	47	43	40
	2	139	185	160	132	107	88	72	61	53	46	41
	3	632	462	346	259	194	146	111	86	68	55	46
	4	632	462	346	259	194	146	111	86	68	55	46
60	1	223	192	168	150	137	125	115	105	95	82	69
	2	240	307	281	246	212	181	154	130	109	90	72
	3	845	673	542	438	354	286	230	184	145	111	82
	4	845	673	542	438	354	286	230	184	145	111	82
90	1	304	270	244	224	208	193	179	166	151	134	116
	2	320	391	365	328	291	256	224	195	168	143	120
	3	939	773	644	538	450	375	310	257	210	168	130
	4	939	773	644	538	450	375	310	257	210	168	130
120	1	374	338	311	289	271	255	239	224	206	186	166
	2	387	458	431	393	354	317	283	252	223	195	169
	3	996	835	709	604	515	438	370	314	263	218	178
	4	996	835	709	604	515	438	370	314	263	218	178

Table 4 shows the average temperature at the effective width of the slab, the temperatures at centers of gravity of bottom and top flanges and at shear connector's mid-height, both as proposed by Eurocode 4 [1] and as calculated by the program. Listed temperatures at the web for the finite element analysis were taken as the average of the values at points 1, 2 and 3.

Table 4 - Temperature evolution for the beam.

	Temperature (^oC)							
Time under fire (min)	30		60		90		120	
	EURO	FEM	EURO	FEM	EURO	FEM	EURO	FEM
Slab (average)	190	128	296	223	361	296	407	356
Bottom flange	364	347	592	552	721	698	780	815
Web	364	292	592	465	721	585	780	675
Top flange	243	132	433	225	573	307	675	376
Connector	194	101	346	186	458	260	540	325
Slab at connector's mid-height	97	66	173	136	229	208	270	271

Table 5 lists the hogging moment design resistance $M_{fi,Rd}$ for the beam, obtained with the assumptions:

- slab temperature taken as the average in Table 4;
- steel profile temperature as given in Table 4.

Table 5 – Hogging moment design resistance (*Mfi,Rd*)

Time (min)	$M_{fi,Rd}$ *(kN.m)*		
	EURO	FEM	EURO/FEM
30	426	426	1.00
60	272	301	0.90
90	128	153	0.84
120	81	102	0.79

5 CONCLUSIONS

For the example proposed in this paper, a verification of table 2 values leads to the following conclusions as to the assumptions of Eurocode 4 [1]:

- results for shear connector temperature match the hypothesis of 80% of the temperature at the top flange of the steel profile (obtained values between 77% and 86%);
- use of 40% of the temperature at the top flange of the steel beam for the concrete slab seems to underestimate actual values, calculated as ranging between 50% and 72%.

Results in table 4 lead to the following conclusions:

- average temperatures at concrete slab were similar for Eurocode and present analyses (32% maximum variation);
- at the bottom flange, FEM calculated temperatures were 3% to 7% lower than when derived by the method proposed by Eurocode 4 [1];
- as for the web, Eurocode results were up to 21% higher;

- for the top flange, finite element analysis resulted in values 44% to 48% lower;
- the same was noted for temperatures at the shear connectors, where computational results were 40% to 48% lower;
- at the slab, temperatures at the connector's mid-height (which serve as reference for these design) were higher for Eurocode (from 0.4% to 32%).

Finally, table 5 shows that the simplifications in Eurocode 4 [1] lead to lower hogging moment design resistance. The finite element results ranged from equal to Eurocode based results for 30 minutes of fire (as the load bearing capacity of the section is not reduced for the resulting temperatures) to a 21% difference after 120 minutes.

REFERENCES

[1] EUROPEAN COMMITTEE FOR STANDARDIZATION, *Design of composite steel and concrete structures. Structural fire design (Part 1.2),* Eurocode 4 – ENV 1994-1-2. Brussels, (1994).

[2] EUROPEAN COMMITTEE FOR STANDARDIZATION, *Basis of design and actions on structures. Actions on structures exposed to fire (Part 2.2)*, Eurocode 1 – ENV 1991-2-2. Brussels , (1995).

[3] EUROPEAN COMMITTEE FOR STANDARDIZATION, *Design of steel structures. General rules and rules for buildings (Part 1.1)*, Eurocode 3 – ENV 1993-3-3. Brussels, (1992).

[4] INTERNATIONAL ORGANIZATION FOR STANDARDIZATION. *Fire resistance tests – Elements of buiding construction*, ISO 834. Geneve, (1994).

[5] F. Zárate and E. Oñate, *Caltep: Programa para el cálculo transitorio de la ecuación de Poisson*, Centro Internacional de Métodos Numéricos em Engenharia, Barcelona, Spain, (1993).

[6] H. Huang and A.S. Usmani, *Finite Element Analysis for Heat Transfer*, Springer-Verlag London Limited. Swansea, UK, (1993).

ACKNOWLEDGMENTS

This project has the support of USIMINAS, CNPq and FAPEMIG. The authors would also like to acknowledge the collaboration of CIMNE.